Higgs Physics at e^+e^- and Photon Colliders

Michael Spira

Paul Scherrer Institut, CH–5232 Villigen PSI, Switzerland

DOI: http://dx.doi.org/10.3204/DESY-PROC-2009-03/Spira

The search for Higgs bosons is one of the most important motivations for future linear e^+e^- and photon colliders. In this contribution the major aspects of Higgs physics of the Standard Model and its minimal supersymmetric extension at these two collider types will be reviewed. In particular the measurements of Higgs masses, quantum numbers and couplings via their production and decay processes at a linear e^+e^- collider will be shortly summarized. Ongoing developments of Higgs boson production via $\gamma\gamma$ fusion and their impact on coupling and parameter measurements will be discussed in detail.

1 Introduction

The Standard Model (SM) predicts the existence of one scalar Higgs boson which constitutes the remainder of electroweak symmetry breaking by means of the Higgs mechanism [1]. The requirement of a weakly interacting SM with a stable vacuum state at the electroweak ground state up to the scale of Grand Unified Theories (GUT), i.e. $\mathcal{O}(10^{16})$ GeV, constrains the Higgs mass to be between 130 and 190 GeV, while lowering this cutoff to the TeV scale enlarges the allowed Higgs mass range to about 50 – 800 GeV [2]. In all experiments this particle has escaped detection so far. The direct search in the LEP2 experiments via the process $e^+e^- \to ZH$ yields a lower bound of 114.4 GeV on the Higgs mass [3]. Electroweak fits to the precision observables at LEP, SLC and the Tevatron colliders yield an upper limit of the Standard Model Higgs mass of about 186 GeV at 95% CL [4].

Due to the hierarchy problem in the context of Grand Unified Theories supersymmetric (SUSY) extensions of the SM are considered as the most attractive solutions. The minimal supersymmetric extension of the SM (MSSM) requires the existence of five elementary Higgs bosons, two neutral CP-even (scalar) bosons h, H, one neutral CP-odd (pseudoscalar) boson A and two charged bosons $H^\pm$. At lowest order all couplings and masses of the MSSM Higgs sector are fixed by two independent input parameters, which are generally chosen as $\tan\beta = v_2/v_1$, the ratio of the two vacuum expectation values $v_{1,2}$, and the pseudoscalar Higgs mass M_A. Including the one-loop and dominant two-loop cor-

Φ		g_u^Φ	g_d^Φ	g_V^Φ
SM	H	1	1	1
MSSM	h	$\cos\alpha/\sin\beta$	$-\sin\alpha/\cos\beta$	$\sin(\beta-\alpha)$
	H	$\sin\alpha/\sin\beta$	$\cos\alpha/\cos\beta$	$\cos(\beta-\alpha)$
	A	$1/\tan\beta$	$\tan\beta$	0

Table 1: MSSM Higgs couplings to SM particles relative to SM Higgs couplings.

rections the upper bound on the light scalar Higgs mass is $M_h \lesssim 135$ GeV [5]. More recent first three-loop results confirm this upper bound within less than 1 GeV [6]. The couplings of the various Higgs bosons to fermions and gauge bosons depend on mixing angles α and β, which are defined by diagonalizing the neutral and charged Higgs mass matrices. They are collected in Table 1 relative to the SM Higgs couplings. For large values of $\tan\beta$ the down-type Yukawa couplings are strongly enhanced, while the up-type Yukawa couplings are suppressed. This feature causes the dominance of bottom-Yukawa-coupling induced processes for large values of $\tan\beta$ at present and future colliders as Higgs decays into bottom quarks and Higgs bremsstrahlung off bottom quarks at hadron and e^+e^- colliders. Moreover, Higgs boson production via gluon fusion $gg \to h, H, A$ is dominated by the bottom-loop contributions for large $\tan\beta$.

Once the Higgs boson of the SM will be found at the LHC, its properties have to be analyzed. However, at the LHC only ratios of Higgs couplings can be determined in the intermediate mass range in a model-independent way. The expected accuracies for the ratios of the various decay channels are displayed in Fig. 1 [7] which implies that a first insight into the fundamental rule $g_i/g_j = m_i/m_j$ for various particles $i, j = W, Z, \tau, b$ can be obtained. For Higgs masses above about 200 GeV the total Higgs decay width can be measured at the LHC with an accuracy down to $\mathcal{O}(10\%)$ for larger Higgs masses, while it is too small to be extracted from the invariant mass peak for smaller Higgs masses [8].

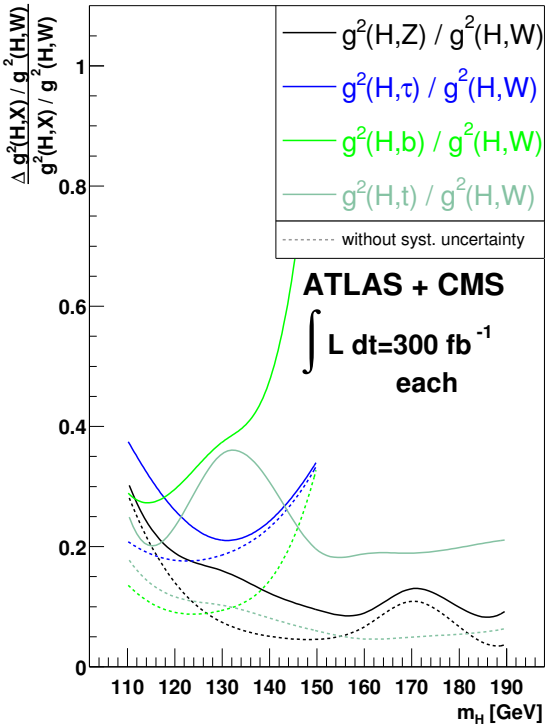

Figure 1: Expected accuracies in measurements of ratios of Higgs couplings at the LHC [7].

A similar situation is expected to emerge for the supersymmetric Higgs bosons of the MSSM in regions where several decay modes of the Higgs particles can be detected. For large values of $\tan\beta$ this fundamental MSSM parameter can be measured with an accuracy at the level of 10% [8]. However, within the MSSM there is a large region for intermediate values of $\tan\beta$ and moderate to large values of the pseudoscalar mass M_A, where the LHC will discover the light scalar Higgs particle h only. Since in this region the light scalar is SM-like it cannot be distinguished from the Higgs boson of the SM. None of the heavier Higgs particles can be seen at the LHC in this wedge region.

2 Higgs Physics at the ILC

Higgs boson production at the ILC proceeds analogously to the LEP collider, i.e. via Higgs-strahlung $e^+e^- \to ZH$ and WW/ZZ–fusion $e^+e^- \to \nu_e\bar{\nu}_e/e^+e^- + H$. The SM Higgs boson can be discovered up to about 70% of the c.m. energy. The Higgs-strahlung process provides the potential to reconstruct the Higgs mass purely from the recoil mass due to the monoenergetic Z boson in the final state and thus independently of the Higgs decay mode. This offers a precise measurement of the Higgs boson mass with an accuracy of 40-80 MeV as is shown in Fig. 2. Moreover, the Higgs boson coupling to the Z boson can be

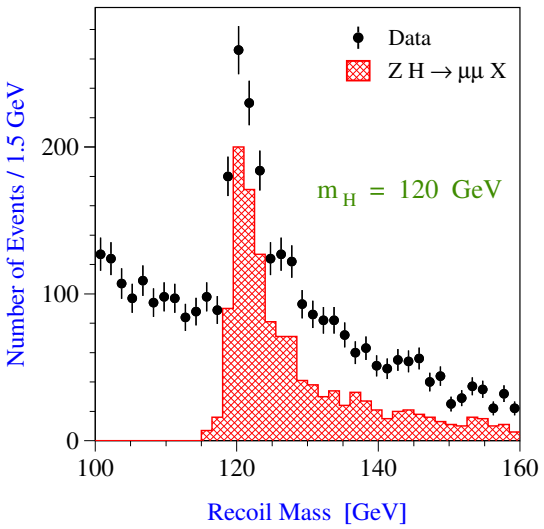

Figure 2: The $\mu^+\mu^-$ recoil mass distribution in the process $e^+e^- \to HZ \to X\mu^+\mu^-$ for $M_H = 120$ GeV and $\int \mathcal{L} = 500 fb^{-1}$ at $\sqrt{s} = 350$ GeV. The dots with error bars are Monte Carlo simulations of the Higgs signal and the background. The shaded histogram represents the signal only. Ref. [9].

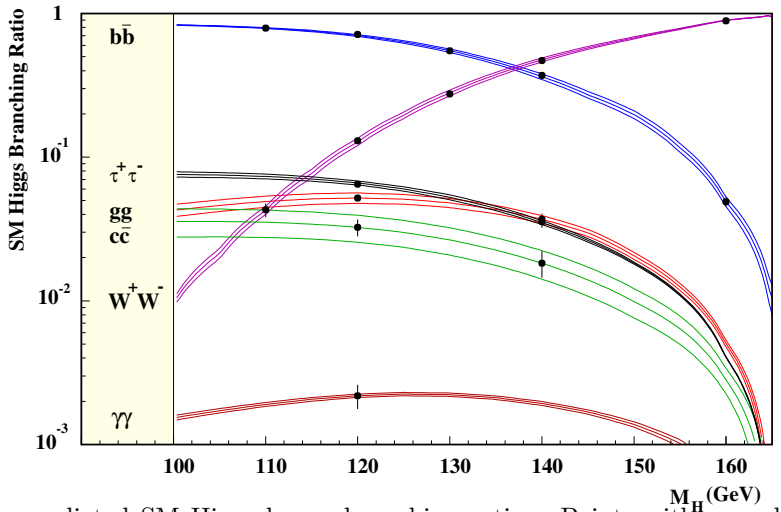

Figure 3: The predicted SM Higgs boson branching ratios. Points with error bars show the expected experimental accuracy, while the lines show the estimated parametric uncertainties on the SM predictions. Ref. [9].

determined in a model-independent manner [9]. This opens the way to a model-independent

measurement of the branching ratios of several Higgs boson decay modes with high accuracy. The results of these studies are displayed in Fig. 3 [9]. These measurements can then be used to determine the corresponding Higgs couplings to bottom and charm quarks, τ leptons as well as to W^+W^-, gg and $\gamma\gamma$ pairs down to the per-cent level in several cases. This completes the picture of the first studies at the LHC with much higher accuracy and with much more model independence.

The angular distribution of the Z/H particles in the Higgs-strahlung process can be used to determine the spin and parity of the Higgs particle as can be inferred from the left plot of Fig. 4. The generic angular distributions of scalar and pseudoscalar Higgs-strahlung differ significantly between each other and from the background of Z boson pair production $e^+e^- \to ZZ$. This can be used to determine the admixture of a pseudoscalar component to the scalar SM Higgs matrix element at the per-cent level [9].

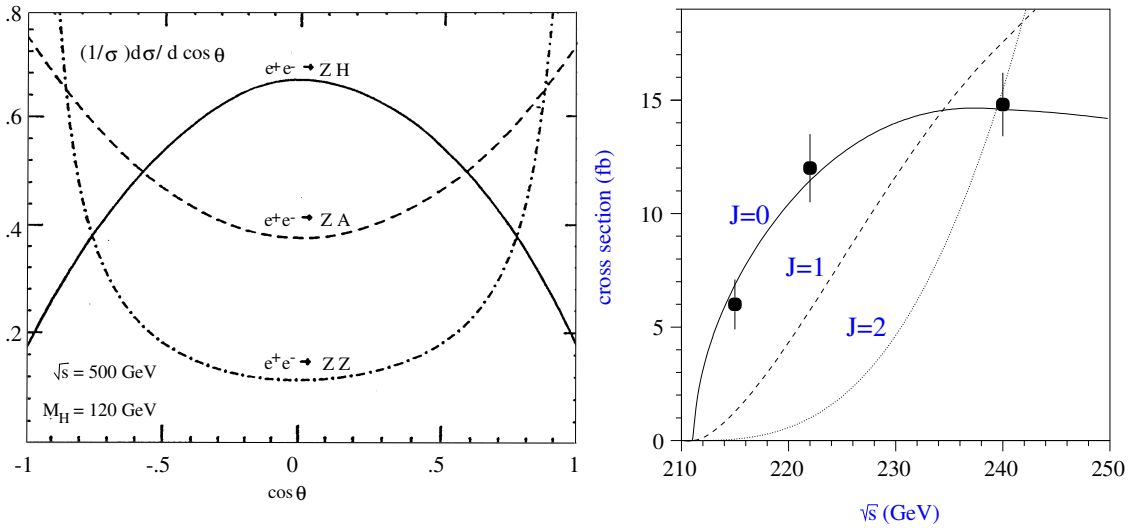

Figure 4: Left: Angular distribution of Z/H bosons in Higgs-strahlung, compared with the production of pseudoscalar particles and the ZZ background final states. Ref. [10]. Right: Threshold excitation of Higgs-strahlung which discriminates spin=0 from other assignments, Ref. [11].

A different method to determine the spin of the Higgs particle is provided by a threshold scan in the Higgs-strahlung process. The theoretical threshold behaviour of particles with different integer spin quantum numbers is shown in the right plot of Fig. 4. The data points reflect the expected accuracies that can be reached at the ILC by a threshold scan [11]. In contrast to the LHC the spin and $\mathcal{CP}$ quantum numbers of the Higgs boson can be uniquely determined at the ILC.

Higgs boson pair production via double Higgs-strahlung $e^+e^- \to ZHH$ and the WW-fusion processes $e^+e^- \to \nu_e\bar{\nu}_e HH$ are sensitive to the trilinear Higgs coupling λ_{HHH}. A measurement of this coupling exhibits the first step towards an experimental measurement of the Higgs potential. This constitutes a crucial test of electroweak symmetry breaking in the Higgs sector. Although the sensitivity of the processes above to λ_{HHH} is quite limited, the experimental accuracy at the ILC with energies up to the TeV range allows a measurement down to the 10%

level in the intermediate Higgs mass range [12] as is shown in Fig. 5.

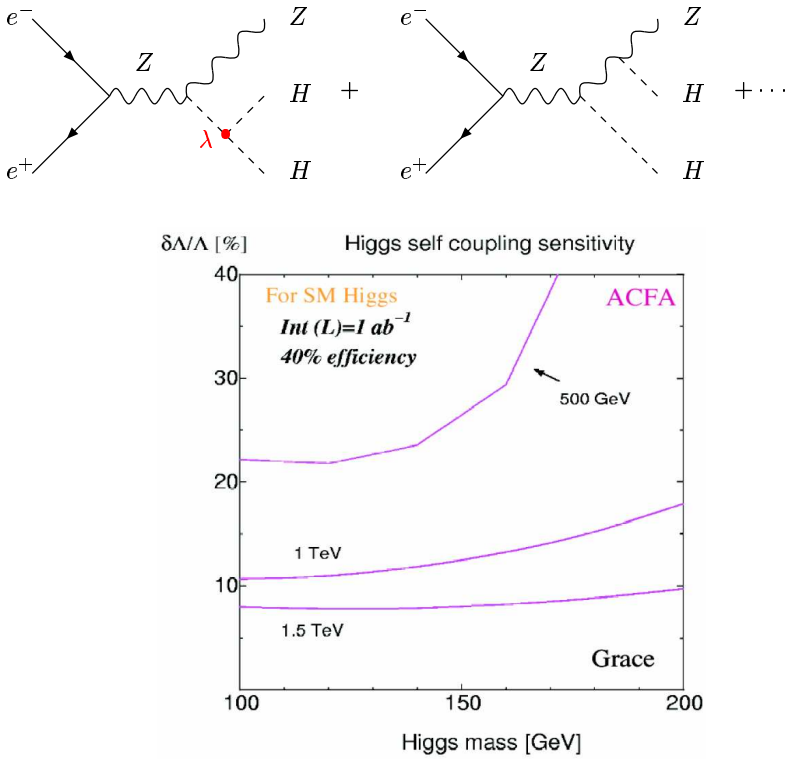

Figure 5: Upper: Generic diagrams of the double Higgs-strahlung process. Lower: The sensitivity of the double Higgs-strahlung and the WW fusion processes to the trilinear Higgs coupling Λ in the intermediate Higgs mass range for an integrated luminosity $\int \mathcal{L} = 1\ ab^{-1}$ at $\sqrt{s} =$ 500 GeV, 1 TeV and 1.5 TeV. Ref. [13].

3 Higgs Physics at the PLC

A photon collider can be constructed on top of the ILC by Compton backscattering of laser light off the e^- beams with a c.m. energy peaking at about 80% of the original e^+e^- energy [14]. This collider mode can be used to search for single s-channel Higgs boson production, since the Higgs particles couple to photon pairs by means of W boson and top/bottom triangle loops. The final state Higgs decay into $b\bar{b}$ pairs can be extracted from the background by appropriate cuts on the bottom scattering angles and by requiring two-jet configurations. In this way the cross section and thus the SM Higgs coupling to photon pairs can be measured with an accuracy at the per-cent level [15], see Fig. 6, for the SM Higgs boson in the intermediate mass range. Since the Higgs coupling to photons develops imaginary parts due to threshold effects inside the loop contributions, it turns out to be complex. The complex phase of the amplitude can be determined from the interference with the ZZ, W^+W^- and $t\bar{t}$ backgrounds at the level of a couple of per-cent at a photon collider [16, 17]. Moreover, the $\mathcal{CP}$ properties of Higgs bosons can

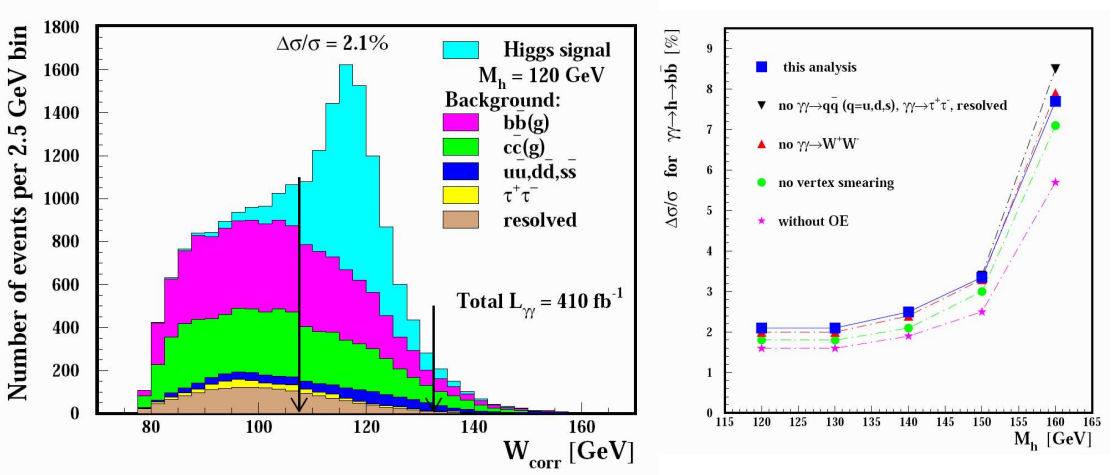

Figure 6: Experimental simulation of the production of SM Higgs bosons with subsequent decay into $b\bar{b}$ at a photon collider. Left: Reconstructed signal peak above backgrounds. Right: Expected accuracy of the cross section measurement. Ref. [15].

be studied at a PLC. The relative $\mathcal{CP}$-phase between the scalar and pseudoscalar components can be measured with an accuracy at the level of a few per-cent in Higgs decays to Z boson pairs [18] and into $t\bar{t}, \tau^+\tau^-$ pairs [17, 19].

The photon collider mode offers the opportunity to produce and search for supersymmetric MSSM Higgs boson in the wedge region in which the LHC can only find the light scalar Higgs boson. Its reach in the $b\bar{b}$ decay channel turns out to be up to about 600 GeV [20], i.e. far beyond the Higgs mass reach of a 500 GeV ILC. Experimental simulations have demonstrated that the production cross section can be measured in this wedge region with a precision at the 10%-level, see Fig. 7. This measurement provides a quantitative test of the photonic MSSM Higgs couplings of the heavy scalar and pseudoscalar Higgs particles, which are sensitive to the heavy charged particle spectrum of the MSSM.

The PLC will allow for a measurement of the trilinear Higgs couplings in Higgs boson pair production processes $\gamma\gamma \to HH$. Generic diagrams contributing to this process are shown in Fig. 8. By tuning the $\gamma\gamma$ c.m. energy according to the Higgs masses an accuracy in the 10% range can be reached at the PLC which is comparable to the accuracies reachable in the e^+e^- mode [21, 22].

Finally, the PLC will provide an additional opportunity to measure the MSSM parameter $\tan\beta$ in the τ-fusion processes $\gamma\gamma \to \tau^+\tau^- + h/H/A \to \tau^+\tau^- b\bar{b}$. By applying proper cuts, the signal processes can be extracted from the background processes which are dominated by $\tau^+\tau^-$ annihilation into bottom quarks and diffractive $\gamma\gamma \to (\tau^+\tau^-)(b\bar{b})$ events. The statistical accuracy, with which large $\tan\beta$ values can be measured, is exemplified for three $\tan\beta$ values in Tab. 2. The scalar and pseudoscalar processes have been combined, whenever the Higgs states are nearly mass degenerate. The absolute errors for the measurement of $\tan\beta$ are of $\mathcal{O}(1)$ which translates into accuracies in the per-cent to 10%-range depending on the size of $\tan\beta$ [23].

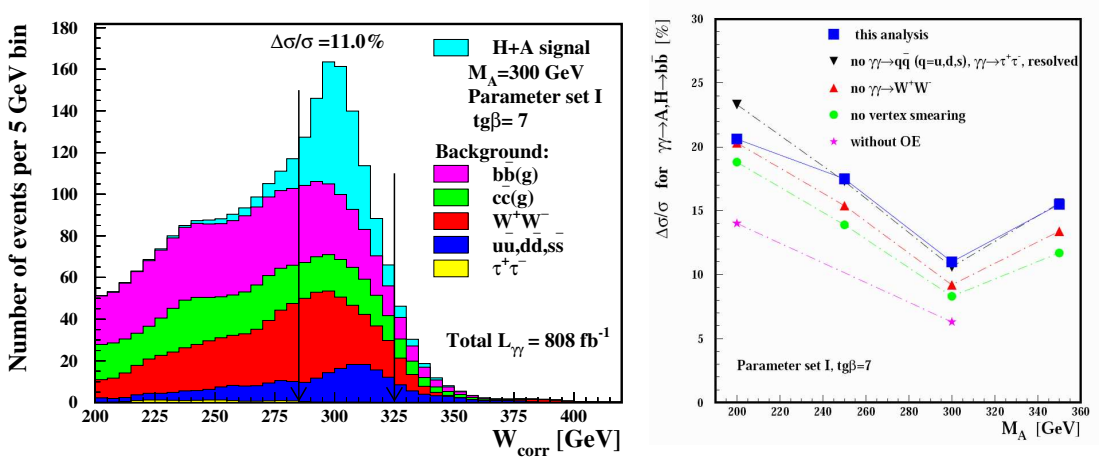

Figure 7: Experimental simulation of the production of heavy MSSM Higgs bosons with subsequent decay into $b\bar{b}$ at a photon collider. Left: Reconstructed signal peak above backgrounds. Right: Expected accuracy of the cross section measurement. Ref. [20].

	$E_{\gamma\gamma} = 400$ GeV, $\mathcal{L} = 100$ fb^{-1}				$E_{\gamma\gamma} = 600$ GeV, $\mathcal{L} = 200$ fb^{-1}				
$\tan\beta$	M_h [GeV]	$A \oplus H : M_A$ [GeV]			$A \oplus H : M_A$ [GeV]				
	100	100	200	300	100	200	300	400	500
10	12.9%	12.8%	10.7%	13.9%	12.3%	9.0%	11.2%	13.2%	16.5%
30	3.7%	3.7%	3.5%	4.6%	3.5%	3.0%	3.7%	4.4%	5.3%
50	2.2%	2.2%	2.1%	2.7%	2.1%	1.8%	2.2%	2.6%	3.2%

Table 2: *Relative errors* $\Delta\tan\beta/\tan\beta$ *on* $\tan\beta$ *measurements for* $\tan\beta = 10$, *30 and 50 based on: h [first column] and combined* $A \oplus H$ *[next three columns] assuming* $E_{\gamma\gamma} = 400$ *GeV,* $\mathcal{L} = 100$ *fb*$^{-1}$, *and* $A \oplus H$ *production [last four columns] with* $E_{\gamma\gamma} = 600$ *GeV,* $\mathcal{L} = 200$ *fb*$^{-1}$. *Ref. [23].*

References

[1] P. W. Higgs, Phys. Lett. **12**, 132 (1964), Phys. Rev. Lett. **13**, 508 (1964) and Phys. Rev. **145**, 1156 (1966); F. Englert and R. Brout, Phys. Rev. Lett. **13**, 321 (1964); G. S. Guralnik, C. R. Hagen and T. W. Kibble, Phys. Rev. Lett. **13**, 585 (1964).

[2] N. Cabibbo, L. Maiani, G. Parisi and R. Petronzio, Nucl. Phys. **B158** (1979) 295; M. Chanowitz, M. Furman and I. Hinchliffe, Phys. Lett. **B78** (1978) 285; R.A. Flores and M. Sher, Phys. Rev. **D27** (1983) 1679; M. Lindner, Z. Phys. **C31** (1986) 295; M. Sher, Phys. Rep. **179** (1989) 273; Phys. Lett. **B317** (1993) 159 and addendum **B331** (1994) 448; G. Altarelli and G. Isidori, Phys. Lett. **B337** (1994) 141; J. Casas, J. Espinosa and M. Quiros, Phys. Lett. **B342** (1995) 171; J. Espinosa and M. Quiros, Phys. Lett. **B353** (1995) 257; A. Hasenfratz, K. Jansen, C. Lang, T. Neuhaus and H. Yoneyama, Phys. Lett. **B199** (1987) 531; J. Kuti, L. Liu and Y. Shen, Phys. Rev. Lett. **61** (1988) 678; M. Lüscher and P. Weisz, Nucl. Phys. **B318** (1989) 705.

[3] G. Abbiendi et al., Phys. Lett. **B565** (2003) 61, [arXiv:hep-ex/0306033].

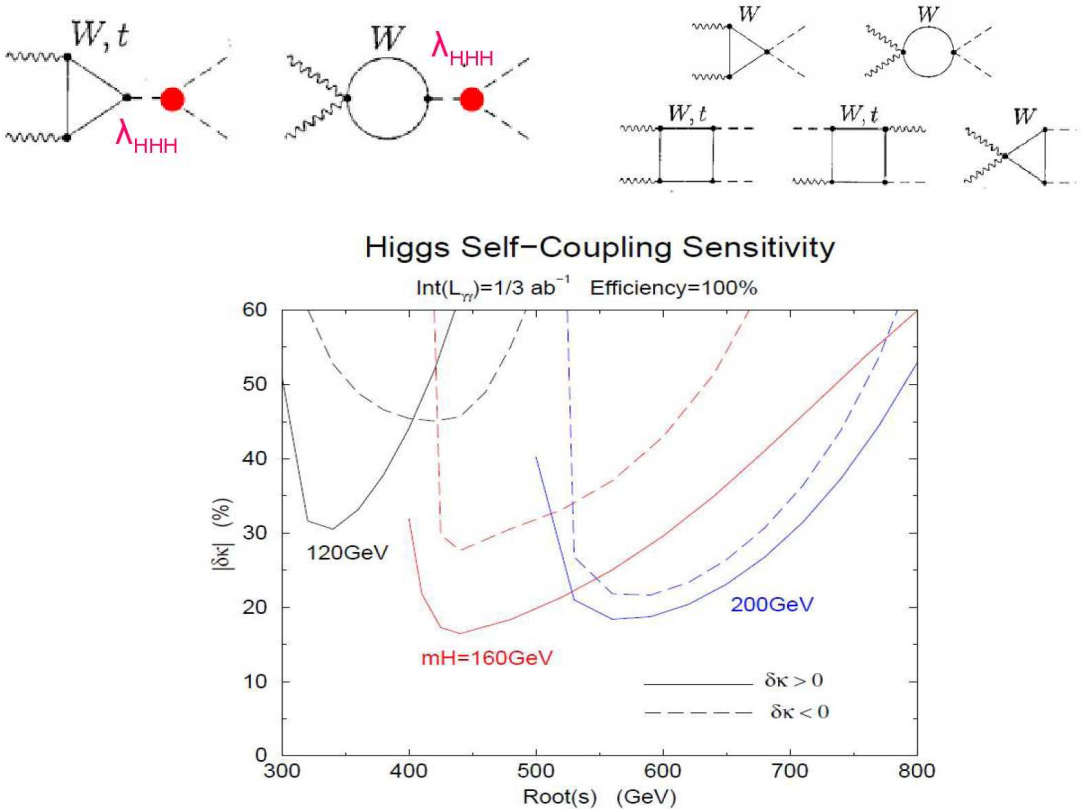

Figure 8: Upper: Generic diagrams contributing to Higgs pair production $\gamma\gamma \to HH$ in the SM. Lower: Experimental sensitivity of SM Higgs boson pair production to the trilinear Higgs coupling κ at a photon collider for different Higgs masses [22].

[4] ALEPH, CDF, D0, DELPHI, L3, OPAL and SLD Collaborations, LEP, SLD and Tevatron Electroweak Working Groups and Heavy Flavour Group, CERN-PH-EP/2008-020, arXiv:0811.4682 [hep-ex].

[5] see e.g. G. Degrassi, S. Heinemeyer, W. Hollik, P. Slavich and G. Weiglein, Eur. Phys. J. **C28** (2003) 133.

[6] S. P. Martin, Phys. Rev. **D75** (2007) 055005; R. V. Harlander, P. Kant, L. Mihaila and M. Steinhauser, Phys. Rev. Lett. **100** (2008) 191602, Erratum *ibid.* **101** (2008) 039901.

[7] M. Dührssen, S. Heinemeyer, H. Logan, D. Rainwater, G. Weiglein and D. Zeppenfeld, Phys. Rev. D **70** (2004) 113009.

[8] ATLAS: Detector and physics performance technical design report, CERN-LHCC-99-014 and CERN–LHCC–99–15; G. L. Bayatian *et al.* [CMS Collaboration], J. Phys. G **34** (2007) 995.

[9] E. Accomando et al., Phys. Rep. **299** (1998) 1; J.A. Aguilar-Saavedra et al., TESLA TDR, hep-ph/0106315; A. Djouadi et al., ILC RDR, arXiv:0709.1893 [hep-ph].

[10] V. Barger, K. Cheung, A. Djouadi, B.A. Kniehl and P. Zerwas, Phys. Rev. **D49** (1994) 79.

[11] D.J. Miller, S.Y. Choi, B. Eberle, M.M. Mühlleitner and P.M. Zerwas, Phys. Lett. **B505** (2001) 149; M.T. Dova, P. Garcia-Abia and W. Lohmann, LC-PHSM-2001-054 [arXiv:hep-ph/0302113].

[12] A. Djouadi, W. Kilian, M. Mühlleitner and P.M. Zerwas, Eur. Phys. J **C10** (1999) 27; M. Mühlleitner, arXiv:hep-ph/0008127; C. Castanier et al., arXiv:hep-ex/0101028, and references in Ref. [9].

[13] GLC project: Linear Collider for TeV physics, KEK-REPORT-2003-7.

[14] I.F. Ginzburg, G.L. Kotkin, V.G. Serbo and V.I. Telnov, Pizma ZhETF **34** (1981) 514, JETP Lett. **34** (1982) 491 and Nucl. Instrum. Meth. **205** (1983) 47; I.F. Ginzburg, G.L. Kotkin, S.L. Panfil, V.G. Serbo and V.I. Telnov, Nucl. Instrum. Meth. **A2** (1984) 5.

[15] G. Jikia, S. Söldner-Rembold, Nucl. Instrum. Meth. A 472 (2001) 133; P. Nieżurawski, A.F. Żarnecki and M. Krawczyk, arXiv:hep-ph/0307183; K. Mönig and A. Rosca, Eur. Phys. J. C **57** (2008) 535.

[16] P. Nieżurawski, A.F. Żarnecki and M. Krawczyk, JHEP **0211** (2002) 034;

[17] E. Asakawa and K. Hagiwara, Eur. Phys. J. C **31** (2003) 351.

[18] S. Y. Choi, D. J. . Miller, M. M. Mühlleitner and P. M. Zerwas, Phys. Lett. B **553** (2003) 61; P. Nieżurawski, A. F. Żarnecki and M. Krawczyk, Acta Phys. Polon. B **36** (2005) 833.

[19] E. Asakawa, S. Y. Choi, K. Hagiwara and J. S. Lee, Phys. Rev. D **62** (2000) 115005; R.M. Godbole, S. Kraml, S.D. Rindani and R.K. Singh, Phys. Rev. D **74** (2006) 095006 [Erratum-ibid. D **74** (2006) 119901].

[20] M. Mühlleitner, M. Krämer, M. Spira, P. Zerwas, Phys. Lett. B 508 (2001) 311; M.M. Mühlleitner, PhD thesis, DESY-THESIS-2000-033, hep-ph/0008127; D. M. Asner, J. B. Gronberg and J. F. Gunion, Phys. Rev. D **67** (2003) 035009; P. Nieżurawski, A.F. Żarnecki and M. Krawczyk, Acta Phys. Polon. B **37** (2006) 1187; M. Spira, P. Nieżurawski, M. Krawczyk and A.F. Żarnecki, Pramana **69** (2007) 931.

[21] R. Belusevic and G. Jikia, Phys. Rev. D **70** (2004) 073017.

[22] E. Asakawa, D. Harada, S. Kanemura, Y. Okada and K. Tsumura, arXiv:0902.2458 [hep-ph].

[23] S. Y. Choi, J. Kalinowski, J. S. Lee, M. M. Mühlleitner, M. Spira and P. M. Zerwas, Phys. Lett. B **606** (2005) 164 and arXiv:hep-ph/0407048.